

2018

Quark Pseudodistributions at Short distances

A. V. Radyushkin

Old Dominion University, aradyush@odu.edu

Follow this and additional works at: https://digitalcommons.odu.edu/physics_fac_pubs



Part of the [Elementary Particles and Fields and String Theory Commons](#)

Repository Citation

Radyushkin, A. V., "Quark Pseudodistributions at Short distances" (2018). *Physics Faculty Publications*. 199.
https://digitalcommons.odu.edu/physics_fac_pubs/199

Original Publication Citation

Radyushkin, A. V. (2018). Quark pseudodistributions at short distances. *Physics Letters B*, 781, 433-442. doi:10.1016/j.physletb.2018.04.023



Quark pseudodistributions at short distances

A.V. Radyushkin ^{a,b,*}

^a Physics Department, Old Dominion University, Norfolk, VA 23529, USA

^b Thomas Jefferson National Accelerator Facility, Newport News, VA 23606, USA

ARTICLE INFO

Article history:

Received 27 October 2017

Received in revised form 28 March 2018

Accepted 11 April 2018

Available online 14 June 2018

Editor: B. Grinstein

ABSTRACT

We perform a one-loop study of the small- z_3^2 behavior of the Ioffe-time distribution (ITD) $\mathcal{M}(v, z_3^2)$, the basic function that may be converted into parton pseudo- and quasi-distributions. We calculate the corrections on the operator level, so that our results may be also used for pseudo-distribution amplitudes and generalized parton pseudodistributions. We separate two sources of the z_3^2 -dependence at small z_3^2 . One is related to the ultraviolet (UV) singularities generated by the gauge link. Our calculation shows that, for a finite UV cut-off, the UV-singular terms vanish when $z_3^2 = 0$. The UV divergences are absent in the reduced ITD given by the ratio $\mathcal{M}(v, z_3^2)/\mathcal{M}(0, z_3^2)$. Still, it has a non-trivial short-distance behavior due to $\ln z_3^2 \Lambda^2$ terms generating perturbative evolution of parton densities. We give an explicit expression, up to constant terms, for the reduced ITD at one loop. It may be used in extraction of PDFs from lattice QCD simulations. We also use our results to get new insights concerning the structure of parton quasi-distributions at one-loop level.

© 2018 The Author. Published by Elsevier B.V. This is an open access article under the CC BY license (<http://creativecommons.org/licenses/by/4.0/>). Funded by SCOAP³.

1. Introduction

The usual parton distribution functions (PDFs) $f(x)$ [1] are often mentioned now as “light-cone PDFs”, since they are related to matrix elements $M(z, p)$ of the $\langle p|\phi(0)\phi(z)|p\rangle$ type taken on the light cone $z^2 = 0$. The parton *pseudo-distributions* $\mathcal{P}(x, -z^2)$ [2,3] generalize PDFs for a situation when z is off the light cone, in particular, when z is spacelike $z^2 < 0$. To obtain them, one should treat $M(z, p)$ as a function $\mathcal{M}(v, -z^2)$ of the Ioffe time $(pz) \equiv -v$ [4] and z^2 . Fourier-transforming $\mathcal{M}(v, -z^2)$ with respect to v gives pseudo-PDFs $\mathcal{P}(x, -z^2)$.

As suggested by X. Ji [5], using purely spacelike separations $z = (0, 0, 0, z_3)$ (or, for brevity, $z = z_3$) allows one to study matrix elements $M(z_3, p)$ (and hence, the Ioffe-time distributions [6] $\mathcal{M}(v, z_3^2)$) on the lattice. To extract PDFs from such studies, one needs to understand the small- z_3^2 behavior of the pseudo-PDFs $\mathcal{P}(x, z_3^2)$.

In any renormalizable theory, a perturbative calculation of the matrix element $M(z_3, p)$ reveals logarithmic $\ln z_3^2$ singularities resulting in the perturbative evolution of PDFs. Further complications arise in quantum chromodynamics (QCD), where the

parton fields are connected by a gauge link $E(0, z; A)$. As emphasized by Polyakov [7], perturbative corrections to gauge links (and loops) result in specific ultraviolet divergences requiring an additional renormalization (see also [8–10]). Studies of the UV and short-distance properties of the QCD bilocal operators $\bar{\psi}(0)\gamma^\alpha E(0, z; A)\psi(z)$ were performed by Craigie and Dorn in Ref. [11] (see also recent papers [12–14]).

An important point is that the effects of perturbative gluon corrections may be formulated on the operator level, without reference to a particular matrix element in which the operator is inserted. This idea is most efficient when realized in the form of the nonlocal (or string) form of light-cone operator product expansion (OPE) [15] that was developed in much detail by Balitsky and Braun [16] who applied it to studies of the light-cone limit. For this reason, they skipped the discussion of the link-specific UV divergences that, at a finite UV cut-off, disappear when $z^2 = 0$. Also, they did not present the z^2 -independent part of the one-loop contribution.

In the present paper, we perform a complete one-loop study of the QCD bilocal operators *off* the light cone. In the context of the quasi-distributions approach [5], the one loop corrections have been recently calculated for quasi-PDFs [17,18], for generalized parton quasi-distributions and for pion quasi-distribution amplitude [19]. All of them result from independent calculations of Feynman diagrams in momentum space, specific for each type of

* Correspondence to: Thomas Jefferson National Accelerator Facility, Newport News, VA 23606, USA.

E-mail address: radyush@jlab.org.

quasi-distributions. The produced results have rather lengthy analytical forms, that strongly differ for each case. In particular, the very question did not arise if, say, the results for the pion quasi-distribution amplitude and quasi-GPDs in Ref. [19] are consistent with the result for the nonsinglet quasi-PDF in Refs. [17,18].

In contrast, using the nonlocal OPE requires just a single calculation of Feynman diagrams. The results obtained in the operator form are rather compact, and may be converted into any parton distribution by a relevant Fourier transform. As examples, we present an expression for the reduced ITD, and we also show how a simple $\ln(z_3^2 m^2)$ evolution logarithm proliferates into a rather complicated structure for quasi-PDF.

Furthermore, working in the coordinate representation allows one to clearly separate UV singular terms from those governed by the evolution effects. We pay a special attention both to the UV-singular link-related contributions and to the UV-finite evolution-related terms singular in the $z_3^2 \rightarrow 0$ limit.

Technically, our calculations are similar to those performed in our paper [20] within the formalism of virtuality distributions [21]. In some aspects, our calculations also resemble those of Ref. [16], where the calculations, however, did not go beyond the leading evolution logarithm.

We start, in Section 2, with a short overview of the basic ideas of our approach formulated in Refs. [22,2]. In Section 3, we outline the nonlocal OPE calculation of the one-loop diagrams in the operator form, and identify the terms responsible for the behavior of the ITD $\mathcal{M}(v, z_3^2)$ for small z_3 . In Section 4, we show that rather simple expressions for the one-loop ITD may be used for a straightforward calculation of the one-loop quasi-PDFs, providing new insights concerning their structure. Section 5 contains the summary of the paper.

2. PDFs

2.1. Ioffe-time distributions

The basic parton distribution functions (PDFs) introduced by Feynman [1] are extracted from the matrix elements of bilocal operators, generically written as $\langle p|\phi(0)\phi(z)|p\rangle$. We use here scalar notations for the partonic fields because complications related to spin are not central to the very concept of PDFs.

In many situations (especially in extraction of parton distributions from the lattice), it is very useful to treat such a matrix element as a function $\mathcal{M}(v, -z^2)$ of two Lorentz invariants, the Ioffe time [4] $(pz) \equiv -v$ and the interval $-z^2$. Thus, we write

$$\begin{aligned} \langle p|\phi(0)\phi(z)|p\rangle &\equiv M(z, p) \\ &= \mathcal{M}(-(pz), -z^2) = \mathcal{M}(v, -z^2). \end{aligned} \quad (2.1)$$

The function $\mathcal{M}(v, -z^2)$ is the Ioffe-time distribution [6].

It can be shown [22,23] that, for all contributing Feynman diagrams, the Fourier transform $\mathcal{P}(x, -z^2)$ of the ITD with respect to v has the $-1 \leq x \leq 1$ support, i.e.,

$$\mathcal{M}(v, -z^2) = \int_{-1}^1 dx e^{ixv} \mathcal{P}(x, -z^2). \quad (2.2)$$

Note that in this covariant definition of x we do not assume that $z^2 = 0$ or $p^2 = 0$.

2.2. Light-cone PDFs

The expressions for various types of parton distributions, all in terms of the same ITD $\mathcal{M}(-(pz), -z^2)$, may be obtained from special choices of z and p . In particular, taking a lightlike z , e.g., that

having the light-front minus component z_- only, we parameterize the matrix element through the twist-2 parton distribution $f(x)$

$$\mathcal{M}(-p_+ z_-, 0) = \int_{-1}^1 dx f(x) e^{-ixp_+ z_-}. \quad (2.3)$$

It has the usual interpretation of probability that the parton carries the fraction x of the target momentum component p_+ . The inverse relation is given by

$$f(x) = \frac{1}{2\pi} \int_{-\infty}^{\infty} dv e^{-ixv} \mathcal{M}(v, 0) = \mathcal{P}(x, 0). \quad (2.4)$$

Since $f(x) = \mathcal{P}(x, 0)$, we may say that the function $\mathcal{P}(x, -z^2)$ generalizes the concept of the usual light-cone parton distribution onto intervals z^2 that are not light-like. The functions $\mathcal{P}(x, -z^2)$ will be referred to as parton pseudo-distributions (or pseudo-PDFs) [2].

2.3. Quasidistributions

Since one cannot have light-like separations on the lattice, it was proposed [5] to consider equal-time separations $z = (0, 0, 0, z_3)$ [or $z = z_3$, for brevity]. Then, in the $p = (E, 0_\perp, P)$ frame, one introduces quasi-PDF $Q(y, P)$ through a parametrization

$$\mathcal{M}(Pz_3, z_3^2) = \int_{-\infty}^{\infty} dy Q(y, P) e^{iyPz_3}. \quad (2.5)$$

The quasi-PDF describes the distribution of parton's $k_3 = yP$ momentum. Using the inverse relation

$$Q(y, P) = \frac{|P|}{2\pi} \int_{-\infty}^{\infty} dz_3 e^{-iyPz_3} \mathcal{M}(Pz_3, z_3^2), \quad (2.6)$$

we can express the quasi-PDF $Q(y, P)$ in terms of the pseudo-PDF $\mathcal{P}(x, z_3^2)$ corresponding to the $z = z_3$ separation

$$Q(y, P) = \frac{|P|}{2\pi} \int_{-1}^1 dx \int_{-\infty}^{\infty} dz_3 e^{-i(y-x)Pz_3} \mathcal{P}(x, z_3^2). \quad (2.7)$$

When $\mathcal{P}(x, z_3^2)$ does not depend on z_3 , i.e., when $\mathcal{P}(x, z_3^2) = f(x)$, the quasidistribution $Q(y, P)$ does not depend on P , and coincides with the PDF $f(y)$.

It should be noted that the integration variable z_3 in Eq. (2.6) enters into both arguments of the ITD $\mathcal{M}(Pz_3, z_3^2)$. In contrast, the pseudo-PDF $\mathcal{P}(x, z_3^2)$ is obtained through integrating the ITD $\mathcal{M}(v, z_3^2)$ just with respect to its first argument,

$$\mathcal{P}(x, z_3^2) = \frac{1}{2\pi} \int_{-\infty}^{\infty} dv e^{-ixv} \mathcal{M}(v, z_3^2). \quad (2.8)$$

2.4. Transverse momentum dependent distributions

If one treats the target momentum p as longitudinal, $p = (E, \mathbf{0}_\perp, P)$, but chooses z that has a transverse $z_\perp = \{z_1, z_2\}$ component, one can introduce the transverse momentum dependent distributions (TMDs). Namely, taking $z_+ = 0$, one defines the TMD $\mathcal{F}(x, k_\perp^2)$ by

$$\mathcal{M}(v, z_{\perp}^2) = \int_{-1}^1 dx e^{ixv} \int_{-\infty}^{\infty} d^2 \mathbf{k}_{\perp} e^{i(\mathbf{k}_{\perp} z_{\perp})} \mathcal{F}(x, k_{\perp}^2). \quad (2.9)$$

One may also write

$$\mathcal{P}(x, z_{\perp}^2) = \int d^2 \mathbf{k}_{\perp} e^{i(\mathbf{k}_{\perp} z_{\perp})} \mathcal{F}(x, k_{\perp}^2). \quad (2.10)$$

This means that the pseudo-PDF $\mathcal{P}(x, z_{\perp}^2)$ coincides in this case with the *impact parameter distribution*, a concept that is well known from TMD studies.

While $z = z_3$ corresponds to a purely “longitudinal” separation, the Lorentz invariance requires that $\mathcal{P}(x, -z^2)$ is the same function of $-z^2$ no matter what kind of a space-like z we deal with. In other words, the dependence of $\mathcal{P}(x, z_3^2)$ on its second argument reflects the same physics that leads to TMDs.

2.5. QCD case

The formulas given above may be used in case of nonsinglet parton densities in QCD. The relevant matrix elements are

$$M^{\alpha}(z, p) \equiv \langle p | \bar{\psi}(0) \gamma^{\alpha} \hat{E}(0, z; A) \psi(z) | p \rangle, \quad (2.11)$$

where $\hat{E}(0, z; A)$ is the standard $0 \rightarrow z$ straight-line gauge link in the quark (fundamental) representation

$$\hat{E}(0, z; A) \equiv P \exp \left[ig z_{\nu} \int_0^1 dt \hat{A}^{\nu}(tz) \right]. \quad (2.12)$$

These matrix elements have p^{α} and z^{α} parts

$$M^{\alpha}(z, p) = 2p^{\alpha} \mathcal{M}_p(-zp, -z^2) + z^{\alpha} \mathcal{M}_z(-zp, -z^2). \quad (2.13)$$

When $z^2 \rightarrow 0$, the \mathcal{M}_p part gives the twist-2 distribution, while \mathcal{M}_z is a purely higher-twist contamination. Note, however, that \mathcal{M}_z does not contribute in the standard definition of unpolarized TMDs because it is based on taking $z = (z_{\perp}, z_{\parallel})$ in the $\alpha = +$ component of \mathcal{O}^{α} . Then the z^{α} -part drops out. As a result, $\mathcal{F}(x, k_{\perp}^2)$ is related to $\mathcal{M}_p(v, z_{\perp}^2)$ by the scalar formula (2.9).

To keep a simple relation between TMDs and z_3 -pseudo-PDFs (and, hence, quasi-PDFs), we need to arrange that the z^{α} contamination does not contribute to pseudo-PDFs. This is achieved by taking the time component of $M^{\alpha}(z = z_3, p)$ and defining

$$M^0(z_3, p) = 2p^0 \mathcal{M}_p(v, z_3^2) = 2p^0 \int_{-1}^1 dx \mathcal{P}(x, z_3^2) e^{ixv}. \quad (2.14)$$

The quasidistribution $Q(y, P)$ is defined in a similar way:

$$M^0(z_3, p) = 2p^0 \int_{-\infty}^{\infty} dy Q(y, P) e^{iyPz_3}. \quad (2.15)$$

As a result, the connection between $Q(y, P)$ and $\mathcal{P}(x, z_3^2)$ is given by the scalar formula (2.7). From now on, we will shorten the notation by using $\mathcal{M}_p \rightarrow \mathcal{M}$.

In QCD, $\mathcal{M}(v, z_{\perp}^2)$ contains $\sim \ln z_{\perp}^2$ terms corresponding to the $\sim 1/k_{\perp}^2$ hard tail of $\mathcal{F}(x, k_{\perp}^2)$. Thus, it makes sense to visualize $\mathcal{M}(v, z_{\perp}^2)$ as a sum of a soft part $\mathcal{M}^{\text{soft}}(v, z_{\perp}^2)$, that has a finite $z_{\perp}^2 \rightarrow 0$ limit, and a logarithmically singular *hard part* reflecting the evolution. The same applies to $\mathcal{M}(v, z_3^2)$.

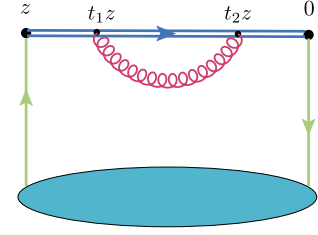


Fig. 1. Renormalization of the gauge link.

3. Hard contribution in coordinate space

Even if one starts with a purely soft TMD (or pseudo-PDF), the gluon exchanges generate the hard part. Our goal is to describe this on the operator level, as a modification of the original soft bilocal operator by gluon corrections.

3.1. Link self-energy contribution

To begin with, we consider the modification resulting from the self-energy correction to the gauge link (see also Refs. [7,24]). At one loop, it is given by

$$\Gamma_{\Sigma}(z) = (ig)^2 C_F \frac{1}{2} \int_0^1 dt_1 \int_0^1 dt_2 z^{\mu} z^{\nu} D_{\mu\nu}^c[z(t_2 - t_1)], \quad (3.1)$$

where $D_{\mu\nu}^c[z(t_2 - t_1)]$ is the gluon propagator connecting points $t_1 z$ and $t_2 z$, see Fig. 1. For massless gluons in Feynman gauge, we have $D_{\mu\nu}^c(z) = -g_{\mu\nu}/4\pi^2 z^2$, and end up with a divergent integral

$$\int_0^1 dt_1 \int_0^1 \frac{dt_2}{(t_2 - t_1)^2}. \quad (3.2)$$

This divergence has an ultraviolet origin. For spacelike z , it may be regularized by using the Polyakov prescription [7] $1/z^2 \rightarrow 1/(z^2 - a^2)$ for the gluon propagator. Taking $z = z_3$ we have

$$\Gamma_{\Sigma}(z_3, a) = -g^2 C_F \frac{z_3^2}{8\pi^2} \int_0^1 dt_1 \int_0^1 \frac{dt_2}{z_3^2 (t_2 - t_1)^2 + a^2}. \quad (3.3)$$

Calculating the integrals gives the result

$$\Gamma_{\Sigma}(z_3, a) = -C_F \frac{\alpha_s}{2\pi} \left[2 \frac{|z_3|}{a} \tan^{-1} \left(\frac{|z_3|}{a} \right) - \ln \left(1 + \frac{z_3^2}{a^2} \right) \right] \quad (3.4)$$

coinciding with that given in Ref. [24].

If we keep z_3 fixed and take the small- a limit, we can expand

$$\Gamma_{\Sigma}(z_3, a)|_{a \rightarrow 0} = -C_F \frac{\alpha_s}{2\pi} \left[\frac{\pi |z_3|}{a} - 2 - \ln \frac{z_3^2}{a^2} + \mathcal{O}(a^2/z_3^2) \right] \quad (3.5)$$

(see also Ref. [12]). This result clearly shows a linear divergence $\sim |z_3|/a$ in the $a \rightarrow 0$ limit. As explained in the pioneering paper [7], it may be interpreted as the mass renormalization δm of a test particle moving along the link,

$$\delta m = C_F \frac{\alpha_s}{2\pi} \frac{\pi}{a}. \quad (3.6)$$

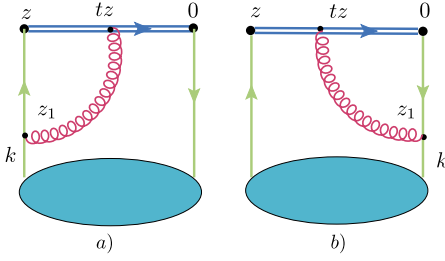


Fig. 2. Insertions of gluons coming out of the gauge link.

Alternatively, for a fixed a and small z_3 , the factor in the square brackets behaves like z_3^2/a^2 , i.e., $\Sigma(z_3, a)$ vanishes at $z_3 = 0$. This distinctive feature of such UV contributions is a mere consequence of the fact that the gauge link converts into unity for $z_3 = 0$.

As a result, the UV terms vanish on the light cone, and that is why they are usually not discussed in the context of the light-cone PDFs. Also, the fact that $\Sigma(z_3 = 0, a) = 0$ means that, at fixed a , Σ gives no corrections to the vector current, i.e. the number of the valence quarks is not changed.

Eq. (3.5) also shows a logarithmic divergence corresponding to the anomalous dimension $2\gamma_{\text{end}}$ due to two end-points of the link. In the lowest order (see, e.g. [10])

$$\gamma_{\text{end}} = -C_F \frac{\alpha_s}{4\pi}. \quad (3.7)$$

In an Abelian theory, the vacuum average of an exponential is the exponential of the one-loop vacuum average. Hence, the one-loop term exponentiates. In the $a \rightarrow 0$ limit, this produces a factor

$$Z_{\text{link}}(z_3, a) = e^{-\delta m|z_3|} e^{-2\gamma_{\text{end}} \ln(z_3^2/a^2)}. \quad (3.8)$$

The exponentiation works also in a non-Abelian case [25–27], but the exponential involves then higher- α_s corrections accompanied by higher irreducible color factors. The all-order renormalization of Wilson loops and lines was discussed in Refs. [8–10].

The Polyakov prescription $1/z_3^2 \rightarrow 1/(z_3^2 + a^2)$ softens the gluon propagator at distances $z_3 \sim$ several a , and eliminates its singularity at $z_3 = 0$. In this respect, it is similar to the UV regularization produced by a finite lattice spacing. Thus, we find it instructive to use this prescription in the studies of the UV properties of pseudo-PDFs.

3.2. Vertex contribution

Working in Feynman gauge, we need also to consider vertex diagrams involving gluons that connect the gauge link with the quarks, see Fig. 2.

3.2.1. Basic structure

There are two possibilities: gluon may be connected to the left (Fig. 2a) or to the right (Fig. 2b) quark leg. To facilitate integration over z_1 , we write the fields at this point in the momentum representation. If the gluon is inserted into the right quark line, we start with

$$O_R^\alpha(z) = (ig)^2 C_F \int_0^1 dt \int d^4 z_1 D^c(z_1 - tz) \times \int d^4 k e^{i(kz_1)} \bar{\Psi}(k) \not{z} S^c(z_1) \gamma^\alpha \psi(z). \quad (3.9)$$

The insertion into the left leg gives a similar expression. Using $S^c(z) = i\not{z}/2\pi^2(z^2)^2$ and $D^c(z) = 1/4\pi^2 z^2$ combined with the representation

$$\frac{1}{(z^2/4)^{N+1}} = \frac{i^{N-1}}{N!} \int_0^\infty d\sigma \sigma^N e^{-i\sigma z^2/4} \quad (3.10)$$

gives a Gaussian integral over z_1 . Taking it, we obtain

$$O_R^\alpha(z) = i \frac{g^2}{8\pi^2} C_F \int_0^1 dt \int_0^\infty d\sigma_1 \frac{d\sigma_1 d\sigma_2}{(\sigma_1 + \sigma_2)^3} \times \int d^4 k e^{i(t(kz)\sigma_2 - \sigma_1 \sigma_2 t^2 z^2/4)/(\sigma_1 + \sigma_2)} \times \bar{\Psi}(k) \left[(kz) + t\sigma_2 z^2/4 \right] \gamma^\alpha \psi(z). \quad (3.11)$$

The external quark lines enter into the soft part, thus we neglect their virtuality, i.e. the k^2 term in the exponential. For the same reason, we also neglect the $\bar{\Psi}(k)\not{k}$ term.

Switching to $\lambda_i = 1/\sigma_i$, introducing common $\lambda = \lambda_1 + \lambda_2$, with $\lambda_1/\lambda = \beta$, then relabeling $\lambda = 1/\sigma$, we obtain

$$O_R^\alpha(z) = i \frac{g^2}{8\pi^2} C_F \int_0^1 dt \int_0^\infty d\sigma e^{-i\sigma t^2 z^2/4} \int_0^1 d\beta \times \int d^4 k e^{i\beta t(kz)} \bar{\Psi}(k) \left[(1-\beta)(kz)/\sigma + t z^2/4 \right] \gamma^\alpha \psi(z). \quad (3.12)$$

3.2.2. UV singular term

We can take the $d^4 k$ integral for the second, namely tz^2 , term in Eq. (3.12) to get

$$O_{R2}^\alpha(z) = i \frac{g^2}{8\pi^2} C_F \int_0^1 dt t \int_0^1 d\beta \times \frac{z^2}{4} \int_0^\infty d\sigma e^{-i\sigma t^2 z^2/4} \bar{\Psi}(t\beta z) \gamma^\alpha \psi(z). \quad (3.13)$$

Now, integration over σ leads to an UV divergence from the small- t integration. The situation is similar to that in the case of the link renormalization. Thus, we regularize $1/z^2 \rightarrow 1/(z^2 - a^2)$ in the initial expression (3.10) for the gluon propagator. Since the singularity is accompanied by the quark field $\bar{\Psi}(t\beta z)$ at $t = 0$, we isolate it by splitting $\bar{\Psi}(t\beta z)$ into $\bar{\Psi}(0) + [\bar{\Psi}(t\beta z) - \bar{\Psi}(0)]$. The UV-singular term is then given by

$$O_{R,\text{UV}}^\alpha(z, a) = \frac{g^2}{8\pi^2} C_F \bar{\Psi}(0) \gamma^\alpha \psi(z) \times \int_0^1 d\beta \int_0^1 dt \frac{tz^2}{t^2 z^2 - a^2/(1-\beta)}. \quad (3.14)$$

Taking integrals over t and β gives the expression

$$O_{R,\text{UV}}^\alpha(z, a) = \frac{g^2}{16\pi^2} C_F \bar{\Psi}(0) \gamma^\alpha \psi(z) \times \left[\left(1 - \frac{a^2}{z^2}\right) \ln \left(1 - \frac{z^2}{a^2}\right) - 1 \right] \quad (3.15)$$

that contains the same $\ln(1 - z^2/a^2)$ logarithmic term as in the self-energy correction (3.4). In the $a \rightarrow 0$ limit, this result agrees with that obtained in Ref. [12]. The diagram with the insertion into the left leg gives the same contribution, thus the total UV-singular contribution doubles $O_{R,\text{UV}}^\alpha(z, a) = 2O_{R,\text{UV}}^\alpha(z, a)$.

Switching to $z = z_3$, we have the $\ln(z_3^2/a^2)$ structure in the $a \rightarrow 0$ limit, and we may combine it with the UV divergences generated by the link self-energy diagrams. Again, for a fixed a , the $O_{UV}^\alpha(z_3, a)$ contribution vanishes in the $z_3^2 \rightarrow 0$ limit.

3.2.3. UV finite term

The $[\bar{\psi}(t\beta z) - \bar{\psi}(0)]$ term vanishes for $t = 0$, and for this reason its contribution

$$O_{R,\text{reg}}^\alpha(z_3, a) = \frac{g^2}{8\pi^2} C_F z_3^2 \int_0^1 dt t \int_t^1 \frac{d\beta}{t^2 z_3^2 + \beta^2 a^2 / (1-\beta)} \times [\bar{\psi}(tz_3)\gamma^\alpha \psi(z_3) - \bar{\psi}(0)\gamma^\alpha \psi(z_3)] \quad (3.16)$$

is finite in the $a \rightarrow 0$ limit. Taking $a = 0$ and integrating over β gives

$$O_{R,\text{reg}}^\alpha(z_3, a = 0) = \frac{\alpha_s}{2\pi} C_F \int_0^1 du \left[\frac{\bar{u}}{u} \right]_+ \bar{\psi}(uz_3)\gamma^\alpha \psi(z_3), \quad (3.17)$$

where we have relabeled $t \rightarrow u$, and introduced $\bar{u} \equiv 1 - u$. The plus-prescription is defined by

$$\int_0^1 du \left[\frac{\bar{u}}{u} \right]_+ F(u) = \int_0^1 du \frac{\bar{u}}{u} [F(u) - F(0)], \quad (3.18)$$

assuming that $F(0)$ is finite. Again, the plus-prescription structure of Eq. (3.17) guarantees that this term gives no corrections to the local current.

Adding the contribution of the diagram with the left-leg insertion, we may write the total regular term as

$$O_{\text{reg}}^\alpha(z_3, a = 0) = \frac{\alpha_s}{2\pi} C_F \int_0^1 du \int_0^1 dv \bar{\psi}(uz_3)\gamma^\alpha \psi(\bar{v}z_3) \times \left\{ \delta(v) \left[\frac{\bar{u}}{u} \right]_+ + \delta(u) \left[\frac{\bar{v}}{v} \right]_+ \right\}. \quad (3.19)$$

In terminology of Balitsky and Braun [16], $\bar{\psi}(uz)\gamma^\alpha \psi(\bar{v}z)$ is a “string operator”. It involves two fields on the straight line segment $(0, z)$, separated from its endpoints by uz and vz , respectively. The difference with Ref. [16] is that z here is not on the light cone $z^2 = 0$.

3.2.4. Evolution terms

Now, let us analyze the $(1-\beta)(kz)/\sigma$ term in Eq. (3.12),

$$O_{R,\text{Evol}}^\alpha(z) = i \frac{g^2}{8\pi^2} C_F \int_0^1 dt \int_0^\infty \frac{d\sigma}{\sigma} e^{-i\sigma t^2 z^2/4} \int_0^1 d\beta (1-\beta) \times \int d^4 k (kz) e^{it\beta(kz)} \bar{\Psi}(k)\gamma^\alpha \psi(z). \quad (3.20)$$

This expression has a logarithmic infrared divergence resulting from the lower limit of the σ integration.

In fact, if we would keep the k^2 term in the exponential of Eq. (3.11), it would produce a $e^{ik^2/\sigma}$ -type factor in the expression above, and there would be no infrared divergence. In other words, the quark virtuality would provide an IR cut-off. In the coordinate representation, this corresponds to a cut-off produced by the nonperturbative z_1^2 -dependence of the soft matrix element $\langle p | \bar{\psi}(0)\gamma^\alpha \psi(z_1) | p \rangle$ (we refer here to Fig. 2a).

An example of calculations, in which such a dependence was taken into account, may be found in our paper [20], where the virtuality distribution formalism was applied to the pion transition form factor. In our present context, the cut-off will be provided by the k_\perp -dependence of the soft part of the TMD $\mathcal{F}(x, k_\perp^2)$, i.e. by the hadron size. Leaving a detailed investigation for future studies, we will just assume now some reasonable form of an IR cut-off function.

In particular, the IR singularity may be regularized by the $e^{-im^2/\sigma}$ factor, which is equivalent to adding the same mass term m^2 to both propagators. In this case (switching to $z^2 = -z_3^2$), we define

$$L_m(t^2 z_3^2 m^2) \equiv \int_0^\infty \frac{d\sigma}{\sigma} e^{i\sigma t^2 z_3^2/4 - im^2/\sigma} = 2K_0(tm|z_3|). \quad (3.21)$$

This function has a logarithmic $\ln z_3^2 m^2$ singularity for small z_3 and an exponential $e^{-|z_3|m}$ fall-off for large z_3 . One should realize that since m parametrizes the IR cut-off imposed by the hadron size, numerically m should be of an order of 0.5 GeV.

Another simple possibility to regularize the IR singularity is to cut the σ -integral from below. Then we have

$$L_{1/z_0}(t^2 z_3^2/z_0^2) \equiv \int_{1/z_0^2}^\infty \frac{d\sigma}{\sigma} e^{i\sigma t^2 z_3^2/4} = \Gamma[0, t^2 z_3^2/4z_0^2], \quad (3.22)$$

where $\Gamma[0, x]$ is the incomplete gamma-function. Again, we have a logarithmic $\ln z_3^2/z_0^2$ singularity for small z_3 , but now a Gaussian $e^{-z_3^2/4z_0^2}$ behavior for large z_3 . As observed in Ref. [20], the two forms of the IR cut-off automatically follow from soft distributions with the exponential and Gaussian fall-off at large z_\perp , respectively.

For small $|z_3|$, we may write in both cases

$$L_\Lambda(t^2 z_3^2 \Lambda^2) = L_\Lambda(z_3^2 \Lambda^2) - 2 \ln t + \mathcal{O}(\Lambda^2 z_3^2). \quad (3.23)$$

The logarithms $\ln(z_3^2 \Lambda^2)$ contained in $L_\Lambda(z_3^2 \Lambda^2)$ reflect the perturbative evolution.

Integrating over t in the part corresponding to the $L_\Lambda(z_3^2 \Lambda^2)$ term in Eq. (3.23), changing the notation $\beta \rightarrow v$, and adding the contribution from the left-leg insertion, we get the total logarithmic contribution coinciding with that of Ref. [16]

$$O_{\log}^\alpha(z_3) = L_\Lambda(z_3^2 \Lambda^2) \frac{\alpha_s}{2\pi} C_F \int_0^1 du \int_0^1 dv \times \left\{ \delta(u) \left[\frac{\bar{v}}{v} \right]_+ + \delta(v) \left[\frac{\bar{u}}{u} \right]_+ \right\} \bar{\psi}(uz_3)\gamma^\alpha \psi(\bar{v}z_3). \quad (3.24)$$

For small z_3^2 , this result corresponds to the following correction to the ITD

$$\mathcal{M}_{\log}(v, z_3^2) = L_\Lambda(z_3^2 \Lambda^2) \frac{\alpha_s}{2\pi} C_F \int_0^1 dw \left[\frac{2w}{1-w} \right]_+ \mathcal{M}^{\text{soft}}(wv, 0). \quad (3.25)$$

Note that, in contrast to the UV divergent contribution, the $L_\Lambda(z_3^2 \Lambda^2)$ function is singular in the $z_3^2 \rightarrow 0$ limit, and the parameter $|z_3|$ in the integrals of Eqs. (3.21), (3.22) works like an ultraviolet rather than an infra-red cut-off.

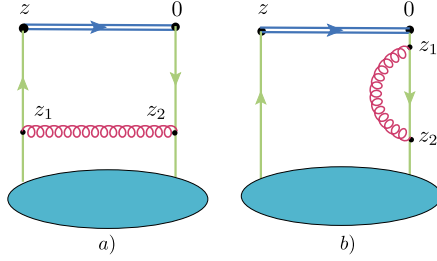


Fig. 3. a) Gluon exchange diagram. b) One of quark self-energy correction diagrams.

3.2.5. IR finite term

The $\ln t$ -term in Eq. (3.23) produces an IR finite contribution

$$O_{\text{R,Fin}}^\alpha(z) = -i \frac{g^2}{4\pi^2} C_F \int_0^1 dt \ln t \int_0^1 d\beta (1-\beta) \times \int d^4k (kz) e^{it\beta(kz)} \bar{\Psi}(k) \gamma^\alpha \Psi(z). \quad (3.26)$$

Transforming the β -integral through integrating exponential by parts, changing $\beta = v/t$ and adding the left $O_{\text{L,Fin}}^\alpha(z)$ contribution, we obtain

$$O_{\text{Fin}}^\alpha(z) = -\frac{\alpha_s}{\pi} C_F \int_0^1 du \int_0^1 dv \bar{\psi}(vz) \gamma^\alpha \psi(\bar{u}z) \times [\delta(u) s_+(v) + \delta(v) s_+(u)], \quad (3.27)$$

where $s_+(u)$ is the plus-prescribed version of $s(u)$ given by

$$s(u) \equiv \int_u^1 dt \frac{\ln t}{t^2} = \frac{1-u + \log(u)}{u}. \quad (3.28)$$

Since this part depends on z through the fields only, we deal with a finite radiative correction to the soft contribution.

3.3. Quark–gluon exchange contribution

There is also a contribution to the hard part given by Fig. 3a containing a gluon exchange between two quark lines. Taking the time component $\alpha = 0$, we have

$$O_{\text{exch}}^0(z_3) = \frac{\alpha_s}{2\pi} C_F \int_0^1 du \int_0^{1-u} dv \times \left\{ L_R(z_3^2 R^2) - 1 \right\} \bar{\psi}(uz_3) \gamma^0 \psi(\bar{v}z_3). \quad (3.29)$$

For the ITD, this gives the integral

$$\mathcal{M}_{\text{exch}}(v, z_3^2) = \frac{\alpha_s}{2\pi} C_F \int_0^1 dw (1-w) \times \left\{ L_R(z_3^2 R^2) - 1 \right\} \mathcal{M}^{\text{soft}}(wv, 0) \quad (3.30)$$

with the $(1-w)$ integrand. Its logarithmic part, combined with the $2w/(1-w)$ term coming from the vertex correction, gives the expected form $(1+w^2)/(1-w)$ [28] of the evolution kernel. Note, however, that unlike the vertex part, the exchange contribution (3.30) does not have the plus-prescription form.

The standard expectation is that one would get it after the addition of the quark self-energy diagrams, one of which is shown

in Fig. 3b. As usual, one should take just a half of each, absorbing the other halves into the soft part. These diagrams have an ultraviolet divergence that may be regularized by the same (for uniformity) Polyakov prescription $1/z^2 \rightarrow 1/(z^2 - a^2)$ for the gluon propagator. The result is a $\ln(a^2 m^2)$ contribution. But, since it has no z -dependence, it cannot help one to get the plus-prescription form for the logarithmic (in z_3^2) part of the exchange contribution.

A possible way out is to represent $\ln(a^2 m^2)$ as the difference $\ln(z_3^2 m^2) - \ln(z_3^2/a^2)$ of the evolution-type logarithm $\ln(z_3^2 m^2)$ and a UV-type logarithm $\ln(z_3^2/a^2)$. The latter can be added to the UV divergences of Figs. 1 and 2, so that the total UV divergent contribution is

$$\Gamma_{\text{UV}}(z_3, a) = -\frac{\alpha_s}{2\pi} C_F \left[2 \frac{|z_3|}{a} \tan^{-1} \left(\frac{|z_3|}{a} \right) - 2 \ln \left(1 + \frac{z_3^2}{a^2} \right) + \frac{1}{2} \ln \left(\frac{z_3^2}{a^2} \right) \right]. \quad (3.31)$$

The $\ln(z_3^2 m^2)$ part should be added to the evolution kernel, and it converts the $(1-w)$ term into $(1-w)_+$.

3.4. Reduced Ioffe-time distribution

Another possibility is to use the reduced Ioffe-time distribution of Refs. [2,3,29,30]

$$\mathfrak{M}(v, z_3^2) \equiv \frac{\mathcal{M}(v, z_3^2)}{\mathcal{M}(0, z_3^2)}. \quad (3.32)$$

Then the UV divergences generated by the link-related and quark self-energy diagrams cancel in the ratio (3.32).¹ Furthermore, since $v=0$ is equivalent to $p=0$, the denominator factor automatically completes the gluon-exchange contribution $(1-w)$ to $(1-w)_+$.

The vertex part (3.25) of the evolution kernel has the plus-prescription structure from the start. For this reason, it does not contribute to the denominator factor $\mathcal{M}(0, z_3^2)$. As a result, $\mathfrak{M}(v, z_3^2)$ satisfies the evolution equation

$$\frac{d}{d \ln z_3^2} \mathfrak{M}(v, z_3^2) = -\frac{\alpha_s}{2\pi} C_F \int_0^1 dw B(w) \mathfrak{M}(wv, z_3^2) \quad (3.33)$$

with respect to z_3^2 , where $B(w)$ is the full plus-prescription Altarelli–Parisi (AP) evolution kernel [28]

$$B(w) = \left[\frac{1+w^2}{1-w} \right]_+. \quad (3.34)$$

The evolution $\ln z_3^2$ dependence of the reduced ITD $\mathfrak{M}(v, z_3^2)$ is clearly visible in the results of the lattice study performed in Ref. [29], where the evolution effects were analyzed within the leading-logarithm approximation (LLA). To go beyond the LLA, one needs also non-logarithmic terms² from (3.19) and (3.27) that contribute to the numerator factor ITD $\mathcal{M}(v, z_3^2)$. However, since they have the plus-prescription structure, they vanish in the denominator factor $\mathcal{M}(0, z_3^2)$. Thus, we get the one-loop expression for the hard part of the reduced ITD in the following form

¹ According to Ref. [12], the cancellation holds to all orders in perturbation theory. See also [13,14], and earlier papers [8–11].

² Such terms also appear in the expression for the pseudo-PDF in Ref. [31]. There is a difference with our results, because its authors use dimensional regularization of IR singularities.

$$\begin{aligned} \mathfrak{M}^{\text{hard}}(\nu, z_3^2) &= -\frac{\alpha_s}{2\pi} C_F \int_0^1 dw \left\{ \left(\frac{1+w^2}{1-w} \right)_+ \left[\ln(z_3^2 m^2 e^{2\gamma_E}/4) + 1 \right] \right. \\ &\quad \left. + 4 \left[\frac{\log(1-w)}{1-w} \right]_+ \right\} \mathfrak{M}^{\text{soft}}(w\nu, 0), \end{aligned} \quad (3.35)$$

where we also have explicitly displayed the logarithmic part of the modified Bessel function $K_0(|z_3|m)$.

4. Hard contribution to quasi-PDFs

The Ioffe-time distributions are basic starting objects for all parton distributions. Hence, the results obtained above may be used to calculate the one-loop corrections for quasi-PDFs. In what follows, we analyze how the z_3^2 -dependence of the one-loop hard part of $\mathcal{M}^{\text{hard}}(\nu, z_3^2)$ is reflected in some specific features of quasi-PDFs. For the soft part, we will assume the collinear approximation $\mathcal{M}^{\text{soft}}(\nu, z_3^2) = \mathcal{M}^{\text{soft}}(\nu, 0)$.

4.1. Ultraviolet divergent terms

For the UV-singular terms, we have

$$\mathcal{M}_{\text{UV}}(\nu, z_3^2) = \Gamma_{\text{UV}}(z_3, a) \mathcal{M}^{\text{soft}}(\nu, 0). \quad (4.1)$$

Combining the definition (2.6) of the quasi-PDFs with the relation (2.4) between $\mathcal{M}(\nu, 0)$ and the PDF $f(x)$ we have

$$Q_{\text{UV}}(y, P) = \int_{-1}^1 dx R_{\text{UV}}(y-x; a) f(x), \quad (4.2)$$

where

$$R_{\text{UV}}(y-x; a) = \frac{P}{2\pi} \int_{-\infty}^{\infty} dz_3 e^{-i(y-x)Pz_3} \Gamma_{\text{UV}}(z_3, a). \quad (4.3)$$

For the link renormalization correction Γ_{Σ} , this Fourier transform can be easily done using its original representation (3.3), producing

$$\begin{aligned} R_{\Sigma}(y, x; Pa) &= \frac{\alpha_s}{2\pi} C_F \frac{1}{Pa} \left[\frac{e^{-|y-x|Pa}}{(y-x)^2} \right. \\ &\quad \left. - \delta(y-x) \int_{-\infty}^{\infty} \frac{d\zeta}{(\zeta-x)^2} e^{-|\zeta-x|Pa} \right]. \end{aligned} \quad (4.4)$$

Note that, due to the exponential suppression factor, the ζ -integral accompanying the $\delta(y-x)$ term converges when $\zeta \rightarrow \pm\infty$. As a result, $R_{\Sigma}(y, x; Pa)$ is given by a mathematically well-defined expression.

The $1/Pa$ term in Eq. (4.4) corresponds to the linear UV divergence. Expanding $e^{-|y-x|Pa}$ in a gives the $1/|y-x|$ term corresponding to the logarithmic $\ln(1+z_3^2/a^2)$ UV divergence in Eq. (3.4). As we have seen, the same $\ln(1+z_3^2/a^2)$ UV contribution appears in the vertex corrections. Calculating the Fourier transform of $\ln(1+z_3^2/a^2)$ gives

$$\begin{aligned} R_V(y, x; Pa) &= -\frac{\alpha_s}{2\pi} C_F \left[\frac{1}{|y-x|} e^{-|y-x|Pa} \right. \\ &\quad \left. - \delta(y-x) \int_{-\infty}^{\infty} \frac{d\zeta}{|y-\zeta|} e^{-|y-\zeta|Pa} \right]. \end{aligned} \quad (4.5)$$

Now we can represent $R_{\Sigma}(y, x; Pa)$ as a sum

$$\begin{aligned} R_{\Sigma}(y, x; Pa) &= \frac{\alpha_s}{2\pi} C_F \left[e^{-|y-x|Pa} \left(\frac{1}{Pa(y-x)^2} + \frac{1}{|y-x|} \right) \right. \\ &\quad \left. - \delta(y-x) \int_{-\infty}^{\infty} d\zeta e^{-|\zeta-x|Pa} \left(\frac{1}{Pa(\zeta-x)^2} + \frac{1}{|\zeta-x|} \right) \right] \\ &\quad + R_V(y, x; Pa), \end{aligned} \quad (4.6)$$

of the regularized $1/(y-x)^2$ singularity corresponding to the linear divergence and the vertex kernel $R_V(y, x; Pa)$ corresponding to the logarithmic divergence.

Here we want to emphasize that keeping the UV regulator nonzero, we get mathematically well-defined expressions that produce the contribution $Q_{\text{UV}}(y, P)$ satisfying

$$\int_{-\infty}^{\infty} dy Q_{\text{UV}}(y, P) = \int_{-\infty}^{\infty} dy \int_{-1}^1 dx R_{\text{UV}}(y-x; a) f(x) = 0, \quad (4.7)$$

and thus not violating the quark number conservation. If one takes $a=0$, the ζ -integrals in Eqs. (4.4) and (4.5) diverge when $\zeta \rightarrow \pm\infty$, and lose mathematical meaning, just like in expressions given in Ref. [17].

One may argue that the limit $a \rightarrow 0$ (or equivalent procedure) should be taken to renormalize UV singularities. Our answer is that one should simply consider the reduced ITD introduced in our paper [2] that does not have the UV divergent terms, so that no UV-renormalization is needed, and the $a \rightarrow 0$ limit poses no problems. Also, the reduced ITD does not produce the problematic $\sim 1/\zeta$ terms in the plus-prescription integrals.

As we will show below, the evolution contribution remaining in the reduced ITD, has $\sim 1/y^2$ behavior for large $|y|$, and the relevant plus-prescription integrals are perfectly convergent for large $|\zeta|$.

4.2. Evolution-related terms

Let us consider now the hard part given by the evolution logarithms

$$\mathcal{M}_{\log}(\nu, z_3^2) = \frac{\alpha_s}{2\pi} C_F L_{\Lambda}(z_3^2 \Lambda^2) \int_0^1 du B(u) \mathcal{M}^{\text{soft}}(u\nu, 0). \quad (4.8)$$

In this case

$$Q_{\log}(y, P) = C_F \frac{\alpha_s}{2\pi} \int_{-1}^1 d\xi f(\xi) \int_0^1 du B(u) K(y-u\xi; \Lambda^2/P^2), \quad (4.9)$$

where the kernel $K(y-u\xi; \Lambda^2/P^2)$ is given by the Fourier transform of $L_{\Lambda}(z_3^2 \Lambda^2)$. If we choose the IR regularization of Eq. (3.21) leading to the modified Bessel function $2K_0(mz_3)$, we have

$$\begin{aligned} K(y-x, m^2/P^2) &= \frac{P}{\pi} \int_{-\infty}^{\infty} dz_3 e^{-i(y-x)Pz_3} K_0(m|z_3|) \\ &= \frac{1}{\sqrt{(y-x)^2 + m^2/P^2}}. \end{aligned} \quad (4.10)$$

We may also write

$$Q_{\log}(y, P) = C_F \frac{\alpha_s}{2\pi} \int_{-1}^1 \frac{d\xi}{|\xi|} R(y/\xi, m^2/\xi^2 P^2) f(\xi), \quad (4.11)$$

where the kernel $R(\eta, m^2/P^2)$ is given by

$$R(\eta; m^2/P^2) = \int_0^1 \frac{du}{\sqrt{(\eta-u)^2 + m^2/P^2}} \left[\frac{1+u^2}{1-u} \right]_+. \quad (4.12)$$

The kernel $R(y/\xi, m^2/\xi^2 P^2)$ in Eq. (4.11) corresponds to a part of the matching factor Z used in the quasi-PDF approach [5]. Note, that its mass-dependence comes through the combination $m^2/\xi^2 P^2$. A similar $\mu^2/\xi^2 P^2$ rescaling was obtained in the recent paper [32], where the dimensional regularization was used as an IR cut-off.

It is convenient to consider the cases $\xi > 0$ and $\xi < 0$ separately. Let us take $\xi > 0$ which corresponds to $f(\xi)$ being nonzero for positive ξ only.

4.2.1. Middle part

Simply taking $m^2/P^2 = 0$ results in a factor $1/|\eta-u|$. When $0 \leq \eta \leq 1$, it produces a non-integrable singularity for $u = \eta$. A more accurate statement is that, with respect to integration over the $0 \leq u \leq 1$ interval, we may represent

$$\frac{1}{\sqrt{(\eta-u)^2 + m^2/P^2}} \Big|_{m^2/P^2 \rightarrow 0} = \left(\frac{1}{|\eta-u|} \right)_+ + \delta(\eta-u) \ln \left[4\eta(1-\eta) \frac{P^2}{m^2} \right], \quad (4.13)$$

where the plus-prescription is defined by

$$\left(\frac{1}{|\eta-u|} \right)_+ = \frac{1}{|\eta-u|} - \delta(\eta-u) \int_0^1 \frac{dv}{|\eta-v|}. \quad (4.14)$$

From the $\delta(\eta-u)$ part we get the evolution term

$$R_1^{\text{middle}}(\eta; m^2/P^2) = \ln \left(\frac{4P^2}{m^2} \right) \left[\frac{1+\eta^2}{1-\eta} \theta(0 \leq \eta \leq 1) \right]_+, \quad (4.15)$$

that is present in the $0 \leq \eta \leq 1$ region only. The remaining $\sim \ln \eta(1-\eta)$ term and terms coming from $(1/|\eta-u|)_+$ are given in this region by

$$R_2^{\text{middle}}(\eta) = \frac{1+\eta^2}{1-\eta} \log[\eta(1-\eta)] + \frac{3/2}{1-\eta} + 4 \frac{\log(1-\eta)}{1-\eta} - 1 + 2\eta. \quad (4.16)$$

4.2.2. Outer parts

For η outside the $0 \leq \eta \leq 1$ segment, the $m^2/P^2 \rightarrow 0$ limit is finite and given by

$$R(\eta; 0)|_{\eta > 1} = \int_0^1 \frac{du}{\eta-u} \left[\frac{1+u^2}{1-u} \right]_+ = - \sum_{n=1}^{\infty} \frac{\gamma_n}{\eta^{n+1}}, \quad (4.17)$$

where γ_n are the anomalous dimensions of operators with n derivatives

$$\gamma_n = \int_0^1 du \frac{1-u^n}{1-u} (1+u^2) = 2 \sum_{j=1}^{n+1} \frac{1}{j} - \frac{3}{2} - \frac{1}{(n+1)(n+2)}. \quad (4.18)$$

At first sight, one would expect a $\sim 1/|\eta|$ behavior for large $|\eta|$. However, the $1/|\eta|$ term is accompanied by the integral of $P(u)$ which vanishes because of the plus-prescription. This is also the reason why γ_0 vanishes causing the series in Eq. (4.17) to start at $n=1$. In a closed form,³

$$R(\eta; 0)|_{\eta > 1} = \frac{1+\eta^2}{\eta-1} \ln \left(\frac{\eta-1}{\eta} \right) + \frac{3}{2(\eta-1)} + 1. \quad (4.19)$$

Similarly, for $\eta < 0$

$$R(\eta; 0)|_{\eta < 0} = \frac{1+\eta^2}{1-\eta} \ln \left(\frac{1-\eta}{-\eta} \right) + \frac{3}{2(1-\eta)} - 1. \quad (4.20)$$

One may notice here the $\pm \frac{3}{2}/(1-\eta)$ terms having the evident $\sim 1/|\eta|$ behavior. But these terms exactly cancel the $\sim 1/|\eta|$ contributions coming from the remaining terms, thus changing the large- η behavior to $\sim 1/\eta^2$. We have already seen the $\sim -1/\eta^2$ asymptotic behavior for $\eta > 1$ in Eq. (4.17). Similarly, for large negative values, one may use the expansion

$$R(\eta; 0)|_{\eta < -1} = \sum_{n=1}^{\infty} \frac{\gamma_n}{\eta^{n+1}}. \quad (4.21)$$

Thus, for large $|\eta|$ we have the asymptotic behavior

$$R(\eta; 0)|_{|\eta| \gg 1} = -\frac{4 \operatorname{sgn}(\eta)}{3} \frac{1}{\eta^2} + \mathcal{O}(1/\eta^3). \quad (4.22)$$

4.3. Quark number conservation

The $\sim 1/y^2$ result for $R(y/\xi; m^2/P^2)$ may be foreseen if one notices that calculating it from the convolution with the AP kernel (see Eq. (4.12)), one deals with the difference

$$\frac{1}{\sqrt{(y-u\xi)^2 + m^2/P^2}} - \frac{1}{\sqrt{(y-\xi)^2 + m^2/P^2}}, \quad (4.23)$$

which behaves like $1/y^2$ for large y . Hence, the integral of $R(y/\xi; m^2/P^2)$ over y does not have divergences for large $|y|$. Moreover, since the two terms differ just by a shift in the y -variable, the integral vanishes. As a result, we have

$$\int_{-\infty}^{\infty} dy R(y/\xi; m^2/P^2) = 0, \quad (4.24)$$

which leads to

$$\int_{-\infty}^{\infty} dy Q_{\log}(y, P) = 0, \quad (4.25)$$

i.e. the evolution part does not change the number of the valence quarks.

³ Comparing our results with those of Ref. [18], one should take into account that the evolution-related contributions are combined there with the UV-singular terms taken in the limit equivalent to our $a \rightarrow 0$.

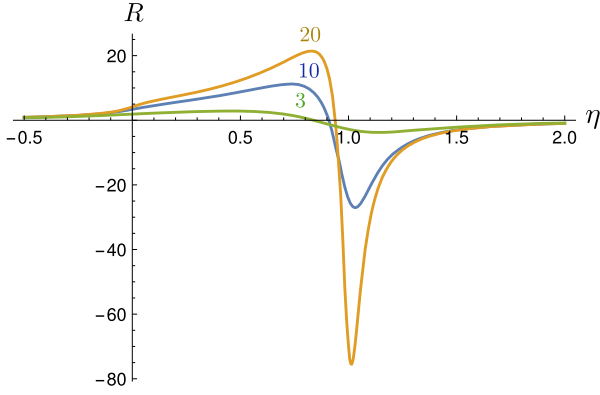


Fig. 4. The kernel $R(\eta, m^2/P^2)$ for $P/m = 3, 10$ and 20 .

4.4. R -kernel at finite momenta

Results for $R(\eta)$ correspond to the full function $R(\eta, m^2/P^2)$ taken in the $P^2/m^2 \rightarrow \infty$ limit. However, since m should be understood as an IR cut-off provided by the hadron size, it has a rather large ~ 0.5 GeV magnitude. On the other hand, the maximal momenta P reached in actual lattice calculations of the quasi-PDFs [33,34] range from 1.3 to about 2.5 GeV. Thus, it is interesting to look at the P/m -dependence of $R(\eta, m^2/P^2)$.

In Fig. 4, we show the structure of the kernel $R(\eta; m^2/P^2)$ for three values of P/m . In the central segment $0 < \eta < 1$, it has the evolution part (4.15) proportional to $\ln(P^2/m^2)$. This term is the main reason for the increase of R with P in this region. A large negative peak in the $y \sim 1$ region also increases its magnitude as $\ln(P^2/m^2)$. It reflects the $\delta(1 - \eta)$ plus-prescription term in the AP kernel.

Note that since the $\ln P^2/m^2$ part (4.15) has the plus-prescription form, its contribution to the integral (4.24) is zero. There are, in addition, non-logarithmic parts (4.16), (4.19), (4.20), and their combined contribution to the integral (4.24) should also vanish. This means that in the $P/m \rightarrow \infty$ limit the negative peak for $\eta = 1$ should contain also a non-logarithmic (in P^2/m^2) part that provides plus-prescription for each of these contributions. For instance, when $\eta > 1$, we would have

$$R(\eta; 0)|_{\eta>1} \rightarrow R(\eta; 0)|_{\eta>1} - \delta(\eta - 1) \int_1^{\infty} d\zeta R(\zeta; 0), \quad (4.26)$$

and similarly for the $0 \leq \eta \leq 1$ and $\eta \leq 0$ parts. The integral over ζ for the $\eta \geq 1$ and $0 \leq \eta \leq 1$ parts diverges when $\zeta \rightarrow 1$, but this is what is expected from the plus-prescription construction. For $\zeta \rightarrow \infty$, the integral converges, hence Eq. (4.26) is a mathematically well-defined expression. For the $\eta \leq 0$ part, the ζ -integral is just a number.

For nonzero m/P , we should have, of course, some smoothed version of $\delta(1 - \eta)$ for the $0 \leq \eta \leq 1$ and $\eta \geq 1$ parts. Looking at the curve corresponding to $P/m = 3$ (the value, realistically corresponding to the momentum $P \sim 1.5$ GeV), one can see that “smoothened” in this case is a strong understatement. This curve does not show anything resembling a delta-function near $\eta = 1$. The reason for a big difference between the finite- P curves and their $P \rightarrow \infty$ limit may be traced to the basic relation (2.6) between quasi-PDFs and pseudo-PDFs: the y -shape of quasi-PDFs $Q(y, P)$ is strongly distorted by the large- z_3 nonperturbative behavior of the pseudo-PDFs $\mathcal{P}(x, z_3^2)$. One needs large momenta P (and some deconvolution techniques) just to get rid of this contaminating large- z_3 information.

In a practical aspect, this means that studying quasi-PDFs at momenta P accessible at present-day lattices, it is a much better approximation to ignore the one-loop corrections rather than to take them in the $m/P \rightarrow 0$ form.

In contrast, if one does not like to use large z_3 values working with the pseudo-PDFs, one can simply exclude them from the analysis. Moreover, since the impact parameter distribution $\mathcal{P}(x, z_3^2)$ of the TMD studies has the same functional form as the pseudo-PDF $\mathcal{P}(x, z_3^2)$, one can use the large- z_3 data to get a direct information about the 3-dimensional hadron structure.

5. Summary

In this paper, we have studied the small- z_3^2 behavior of the Ioffe-time distribution $\mathcal{M}(v, z_3^2)$ at one-loop level. The ITD is the basic function that may be converted, in a prescribed way, into pseudo-PDFs and quasi-PDFs. In its turn, the short-distance structure of the ITD is determined by that of the underlying bilocal operator $\mathcal{O}^\alpha(0, z) = \bar{\psi}(0)\gamma^\alpha E(0, z; A)\psi(z)$. Since the corrections to $\mathcal{O}^\alpha(0, z)$ may be calculated on the operator level, it is an even more fundamental object.

In our study, we made an effort to separate two sources of the z_3^2 -dependence at small z_3^2 . One is related to the UV singularities generated by the gauge link $E(0, z_3; A)$ connecting the quark fields forming the QCD bilocal operator. The logarithmic part of these terms has the $\ln(1 + z_3^2/a^2)$ structure, where a is the UV cut-off parameter analogous to lattice spacing. Thus, while being singular in the $a \rightarrow 0$ limit, the $\ln(1 + z_3^2/a^2)$ factor vanishes for $z_3^2 = 0$. This is a general property of the link-related UV-singular terms. This property is a very important one since it guarantees that such corrections do not change the number of valence quarks.

The one-loop UV divergences are eliminated if one considers the reduced ITD $\mathfrak{M}(v, z_3^2)$ given by the ratio $\mathcal{M}(v, z_3^2)/\mathcal{M}(0, z_3^2)$. Still, $\mathfrak{M}(v, z_3^2)$ has a non-trivial short-distance behavior. At one loop, it has the $\ln z_3^2 \Lambda^2$ structure, where Λ is an IR cut-off parameter. These terms generate perturbative evolution of the parton densities. While they are singular in the $z_3^2 \rightarrow 0$ limit, the evolution corrections do not change the number of valence quarks. This is secured by the fact that the v -dependence of such corrections is governed by factors possessing the plus-prescription property. The explicit expression that we give for the z_3^2 -dependence of the reduced ITD at one loop, may (and will) be used in our future work on extraction of PDFs from the lattice QCD simulations using the pseudo-PDF-based methodology.⁴

We have also demonstrated that our results may be used for a rather straightforward calculation of the one-loop corrections to quasi-PDFs, providing new insights concerning their structure. In particular, we have demonstrated that keeping a nonzero UV regulator a , one can obtain mathematically well-defined expressions for quasi-PDFs, involving the plus-prescription integrals that do not diverge at infinity.

For the UV-finite evolution part, we have demonstrated that they produce quasi-PDFs with $\sim 1/y^2$ behavior that also results in convergent plus-prescription integrals. We have also observed that the mass-dependence of the matching kernel, that relates quasi-PDFs with the ordinary collinear PDFs $f(\xi)$, comes through the $m^2/\xi^2 P^2$ combination.

We have also argued that the IR scale m should be treated as a parameter whose size is of an order of the inverse hadron radius $1/R \sim 0.5$ GeV. As a result, for presently accessible hadron momenta P , the one-loop corrections for quasi-PDFs are much smaller than in the formal $m/P \rightarrow 0$ limit.

⁴ These results have been already used for such a study in our recent paper [35].

As emphasized above, the corrections to the bilocal operator $\mathcal{O}^\alpha(0, z)$ may be calculated without specifying a matrix element in which it is embedded. In particular, changing the $\langle p | \dots | p \rangle$ brackets into $\langle 0 | \dots | p \rangle$, one may use the results of the present paper to get one-loop corrections to pseudo- and quasidistribution amplitudes. Similarly, taking the $\langle p_1 | \dots | p_2 \rangle$ matrix elements, one can get one-loop results for generalized parton pseudodistributions (“pseudo-GPDs”). These are natural directions for future studies.

Acknowledgements

I thank I. Balitsky, V.M. Braun, L. Jin, J.-W. Qiu and Y. Zhao for discussions and K. Orginos for his interest in this work. This work is supported by Jefferson Science Associates, LLC under U.S. DOE Contract #DE-AC05-06OR23177 and by U.S. DOE Grant #DE-FG02-97ER41028.

References

- [1] R.P. Feynman, *Photon–Hadron Interactions*, Reading, 1972, 282 pp.
- [2] A.V. Radyushkin, *Phys. Rev. D* 96 (3) (2017) 034025.
- [3] A. Radyushkin, arXiv:1711.06031 [hep-ph].
- [4] B.L. Ioffe, *Phys. Lett. B* 30 (1969) 123.
- [5] X. Ji, *Phys. Rev. Lett.* 110 (2013) 262002.
- [6] V. Braun, P. Gornicki, L. Mankiewicz, *Phys. Rev. D* 51 (1995) 6036.
- [7] A.M. Polyakov, *Nucl. Phys. B* 164 (1980) 171.
- [8] V.S. Dotsenko, S.N. Vergeles, *Nucl. Phys. B* 169 (1980) 527.
- [9] R.A. Brandt, F. Neri, M.a. Sato, *Phys. Rev. D* 24 (1981) 879.
- [10] S. Aoyama, *Nucl. Phys. B* 194 (1982) 513.
- [11] N.S. Craigie, H. Dorn, *Nucl. Phys. B* 185 (1981) 204.
- [12] T. Ishikawa, Y.Q. Ma, J.W. Qiu, S. Yoshida, *Phys. Rev. D* 96 (9) (2017) 094019.
- [13] X. Ji, J.H. Zhang, Y. Zhao, arXiv:1706.08962 [hep-ph].
- [14] J. Green, K. Jansen, F. Steffens, arXiv:1707.07152 [hep-lat].
- [15] S.A. Anikin, O.I. Zavvalov, *Ann. Phys.* 116 (1978) 135.
- [16] I.I. Balitsky, V.M. Braun, *Nucl. Phys. B* 311 (1989) 541.
- [17] X. Xiong, X. Ji, J.H. Zhang, Y. Zhao, *Phys. Rev. D* 90 (1) (2014) 014051.
- [18] X. Ji, J.H. Zhang, *Phys. Rev. D* 92 (2015) 034006.
- [19] X. Ji, A. Schäfer, X. Xiong, J.H. Zhang, *Phys. Rev. D* 92 (2015) 014039.
- [20] A.V. Radyushkin, *Phys. Rev. D* 93 (5) (2016) 056002.
- [21] A.V. Radyushkin, *Phys. Lett. B* 735 (2014) 417.
- [22] A. Radyushkin, *Phys. Lett. B* 767 (2017) 314.
- [23] A.V. Radyushkin, *Phys. Lett. B* 131 (1983) 179.
- [24] J.W. Chen, X. Ji, J.H. Zhang, *Nucl. Phys. B* 915 (2017) 1.
- [25] J.G.M. Gatheral, *Phys. Lett. B* 133 (1983) 90.
- [26] J. Frenkel, J.C. Taylor, *Nucl. Phys. B* 246 (1984) 231.
- [27] G.P. Korchemsky, A.V. Radyushkin, *Nucl. Phys. B* 283 (1987) 342.
- [28] G. Altarelli, G. Parisi, *Nucl. Phys. B* 126 (1977) 298.
- [29] K. Orginos, A. Radyushkin, J. Karpie, S. Zafeiropoulos, *Phys. Rev. D* 96 (9) (2017) 094503.
- [30] J. Karpie, K. Orginos, A. Radyushkin, S. Zafeiropoulos, arXiv:1710.08288 [hep-lat].
- [31] X. Ji, J.H. Zhang, Y. Zhao, *Nucl. Phys. B* 924 (2017) 366.
- [32] T. Izubuchi, X. Ji, L. Jin, I.W. Stewart, Y. Zhao, arXiv:1801.03917 [hep-ph].
- [33] H.W. Lin, J.W. Chen, S.D. Cohen, X. Ji, *Phys. Rev. D* 91 (2015) 054510.
- [34] C. Alexandrou, K. Cichy, M. Constantinou, K. Hadjiyiannakou, K. Jansen, F. Steffens, C. Wiese, *Phys. Rev. D* 96 (1) (2017) 014513.
- [35] A. Radyushkin, arXiv:1801.02427 [hep-ph].